ARTHRITIS & RHEUMATISM
Vol. 62, No. 12, December 2010, pp 3695–3705
DOI 10.1002/art.27710

Characterization of the Human Nucleus Pulposus Cell Phenotype and Evaluation of Novel Marker Gene Expression to Define Adult Stem Cell Differentiation

Ben M. Minogue, Stephen M. Richardson, Leo A. H. Zeef, Anthony J. Freemont, and Judith A. Hoyland

Objective. **Development of stem cell therapies for regenerating the nucleus pulposus (NP) are hindered by the lack of specific markers by which to distinguish NP cells from articular chondrocytes (ACs). The purpose of this study was to define the phenotype profile of human NP cells using gene expression profiling and to assess whether the identified markers could distinguish mesenchymal stem cell (MSC) differentiation to a correct NP cell phenotype.**

Methods. **Affymetrix MicroArray analyses were conducted on human NP cells and ACs, and differential expression levels for several positive (NP) and negative (AC) marker genes were validated by real-time quantitative polymerase chain reaction (PCR) analysis. Novel marker gene and protein expression was also assessed in human bone marrow–derived MSCs (BM-MSCs) and adipose tissue–derived MSCs (AD-MSCs) following differentiation in type I collagen gels.**

Results. **Analysis identified 12 NP-positive and 36-negative (AC) marker genes that were differentially expressed ≥20-fold, and for a subset of them (NP-positive genes *PAX1*, *FOXF1*, *HBB*, *CA12*, and *OVOS2*; AC-positive genes *GDF10*, *CYTL1*, *IBSP*, and *FBLN1*), differential expression was confirmed by real-time quantitative PCR. Differentiated BM-MSCs and AD-MSCs demonstrated significant increases in the novel NP markers *PAX1* and *FOXF1*. AD-MSCs lacked expression of the AC markers *IBSP* and *FBLN1*, whereas BM-MSCs lacked expression of the AC marker *IBSP* but expressed *FBLN1*.**

Conclusion. **This study is the first to use gene expression profiling to identify the human NP cell phenotype. Importantly, these markers can be used to determine the in vitro differentiation of MSCs to an NP-like, rather than an AC-like, phenotype. Interestingly, these results suggest that AD-MSCs may be a more appropriate cell type than BM-MSCs for use in engineering intervertebral disc tissue.**

Low back pain is a major public health problem in the Western World, with over 80% of the population estimated to report low back pain during their lifetime (1). This has a serious impact on economies, with total costs related to this condition exceeding $100 billion per year in the US alone (2). One of the principal causes of low back pain is degeneration of the intervertebral disc (IVD), whereby adverse changes in the matrix results in dehydration of the nucleus pulposus (NP), loss of disc height, and loss of mechanical function, leading to traumatic damage and associated pain (3–5).

Current treatments are aimed at relieving symptoms of low back pain, rather than halting progression of the disease by inhibiting the underlying disease mechanisms or by restoring disc structure and function. Thus, there is an urgent need to provide more-effective treatments for IVD degeneration. Since the NP is the region of the IVD that is most affected during degeneration,

Supported by Arthritis Research UK (grant 18046). The Intervertebral Disc Group within the University of Manchester School of Biomedicine is supported by the Manchester Academic Health Sciences Centre and the National Institute for Health Research, Manchester Biomedical Research Centre.

Ben M. Minogue, PhD, Stephen M. Richardson, PhD, Leo A. H. Zeef, PhD, Anthony J. Freemont, MD, FRCP, FRCPath, Judith A. Hoyland, PhD: University of Manchester, Manchester, UK.

Drs. Minogue and Richardson contributed equally to this work.

Address correspondence and reprint requests to Judith A. Hoyland, PhD, School of Biomedicine, The University of Manchester, Stopford Building, Oxford Road, Manchester M13 9PT, UK. E-mail: Judith.hoyland@manchester.ac.uk.

Submitted for publication April 6, 2010; accepted in revised form August 10, 2010.

the focus of many recent studies has been on the use of cell-based tissue engineering to regenerate the NP. Indeed, a number of recent advances in IVD and stem cell biology have demonstrated that both bone marrow–derived mesenchymal stem cells (BM-MSCs) and adipose tissue–derived mesenchymal stem cells (AD-MSCs) are capable of differentiating into chondrocyte-like cells of the NP in vitro (6–10) and in vivo in animal models (11–13). This offers the realistic hope of providing cellular therapies that will restore functional IVD tissue in degenerated discs.

In order to ensure a successful clinical outcome for any stem cell–based tissue engineering strategy, however, it is essential that implanted cells adopt the correct phenotype. Given the similarities in phenotype between NP cells and articular chondrocytes (ACs) (14), many studies have used a small panel of communally expressed markers, including *SOX9*, *COL2A1*, and *ACAN* to identify an NP cell (14–16). However, there are clear morphologic and physiologic differences between articular cartilage and NP tissues, suggesting that there are differences in their cellular phenotypes and that the identification of the exact phenotype for NP cells is essential for ensuring the correct cell type is obtained and that, ultimately, the appropriate extracellular matrix is produced.

There have, however, been surprisingly few attempts to characterize the differences between the molecular phenotypes of NP and AC cells, although a small number of recent studies have used microarray technology to compare the gene expression profiles of IVDs and ACs in rat, canine, and bovine tissues (17–20) or have used proteomic technology to compare proteins in bovine NP cells and ACs (21). Lee et al (18) identified *KRT19* and *GPC3* as being differentially expressed genes that also stained immunopositive in the NP of discs from young rats but were negative in the anulus fibrosus (AF) and articular cartilage. They also identified *A2M*, *KRT18*, and *NCAM1* as being enhanced in NP cells as compared with ACs from canine tissues (20). However, when the same group of investigators examined the expression of their rat markers in canine tissues, they found that only 2 AC markers (*COMP* and *MGP*) demonstrated a similar pattern, highlighting the importance of identifying gene markers that are both cell-specific and species-specific when defining the NP phenotype.

For human tissue regeneration and engineering purposes, it is essential that genes identified in animals can be applied to human NP cells. A recent study compared rat and canine marker genes identified by microarray analysis to human IVD and cartilage tissues and concluded that only *KRT19* has the potential to characterize human NP cells (22), although interestingly, the expression of this marker was lost by the age of 45, suggesting that it is more indicative of a young or nondegenerated NP phenotype. Our group of investigators has also recently identified novel marker genes that were differentially expressed in bovine IVD cells and ACs and examined their suitability for the identification of human NP cells (19). Data showed that the majority of these genes were differentially expressed to a lesser degree in humans, again illustrating species variation. It is therefore imperative that for definitive characterization of a human NP cell phenotype, microarray studies should be undertaken with human tissues to produce a comprehensive molecular signature, which will enable researchers to more accurately distinguish an NP cell from an AC. Thus, the aims of this study were to conduct microarray experiments using human ACs and NP cells to identify NP- and AC-specific markers, and to use these markers to identify the phenotype of both BM-MSCs and AD-MSCs differentiated in vitro in biomaterials for potential use in IVD tissue engineering.

MATERIALS AND METHODS

Human tissues and sample preparation. Human IVD tissues were obtained from tissue donors during postmortem examination, with informed consent from the donor's relatives and with the approval of the North West Research Ethics Committee. All postmortem samples were obtained from donors who died of natural causes (e.g., heart failure), had no history of back pain, and had no other relevant clinical history, such as bone metastases. Representative tissue samples were processed to paraffin wax embedding for grading according to a published 12-point histologic scale (14). The remaining disc tissue was macroscopically dissected.

Human articular cartilage samples were obtained during total knee arthroplasty in osteoarthritis (OA) patients, with the informed consent of the patients and with approval of the South Manchester Research Ethics Committee. Samples with a "normal" macroscopic appearance were harvested, and full-thickness sections (excluding subchondral bone) were processed to paraffin wax embedding for grading according to a published 11-point histologic scoring system adapted from Mankin et al (23), as previously described (24).

Only NP and cartilage samples that were histologically graded as "normal" were used. Each tissue sample was dissected into 2–3-mm^3 fragments, placed on an orbital shaker at 37°C, and enzymatically digested for 1 hour in serum-free medium containing 0.5% Pronase (Calbiochem) and then for 2–3 hours in 0.5% type II collagenase (Invitrogen) and 0.1% hyaluronidase (Sigma). Cells were passed through a 40-μm filter, collected by centrifugation at 500*g* for 5 minutes, and then lysed in TRIzol reagent (Invitrogen).

RNA was extracted according to the manufacturer's

Table 1. Human oligonucleotide primers used for real-time quantitative polymerase chain reaction analysis

Gene name	Gene symbol	NCBI RefSeq	Forward primer	Reverse primer
Glyceraldehyde-3-phosphate dehydrogenase	*GAPDH*	NM_002046.3	GCACCGTCAAGGCTGAGAAC	GGATCTCGCTCCTGGAAGATG
Aggrecan	*ACAN*	NM_001135.2	TCTACCGCTGCGAGGTGAT	TGTAATGGAACACGATGCCTTT
Type II collagen α1	*COL2A1*	NM_001844.4	GGAAGAGTGGAGACTACTGGATTGAC	TCCATGTTGCAGAAAACCTTCA
Hemoglobin β-chain	*HBB*	NM_000518.4	CACCTTTGCCACACTGAGTGA	GTGATGGGCCAGCACACA
Carbonic anhydrase XII	*CA12*	NM_001218.3	CGTGCTCCTGCTGGTGATCT	AGTCCACTTGGAACCGTTCACT
Ovostatin 2	*OVOS2*	XM_002343151.1	CCTCCAAGCAGGGAGTTTTG	TATCCCCCACAACAGTGAAAAAG
Paired box 1	*PAX1*	NM_006192.3	TGGCCCTCGGCTCATTC	GCCCCTGTTTGCTCCATAAA
Forkhead box F1	*FOXF1*	NM_001451.2	AAGCCGCCCTATTCCTACATC	GCGCTTGGTGGGTGAACT
Integrin-binding sialoprotein (bone sialoprotein 2)	*IBSP*	NM_004967.3	CCAGAGGAAGCAATCACCAAA	GCACAGGCCATTCCCAAA
Fibulin 1	*FBLN1*	NM_006487.2	CCTTCGAGTGCCCTGAGAACTA	ACCGATGGCCTCATGCA
Growth differentiation factor 10	*GDF10*	NM_004962.2	TGCCTAAGATCGTTCGTCCAT	CCCAAGGGAGTTCATCTTATCG
Cytokine-like 1	*CYTL1*	NM_018659.2	GGCTGTACCTGGACATACACAATTACT	GGGCGAGGCCACAAAGT

instructions and was quantified using a NanoDrop ND-1000 spectrophotometer (NanoDrop Technologies). Quality was checked by means of an RNA 6000 NanoAssay on an Agilent 2100 Bioanalyzer.

Complementary DNA (cDNA) microarrays. To minimize the effect of biologic variation on differential expression, hybridizations for each cell type from 3 separate individuals were performed in triplicate. Only high-quality RNA with an RNA integrity number of at least 7 taken from 3 histologically "normal" IVD samples (2 male and 1 female donor, ages 46–57 years [mean age 51 years]; histologic grade 1 or 2) and articular cartilage samples (1 male and 2 female donors, ages 55–60 years [mean age 58 years]; Mankin grade 1 or 2) were used for the microarrays.

For each hybridization, 100 ng of total RNA was used in the Affymetrix GeneChip Two-Cycle Target Labeling kit and in the Ambion MEGAscript T7 kit before hybridizing to the GeneChip human genome U133 Plus 2.0 array (Affymetrix) according to manufacturer's instructions. Technical quality control was performed with dChip software (25). Background correction, quantile normalization, and gene expression analysis were performed using the robust multiarray average (RMA) analysis in the Bioconductor software package (26). Differential expression analysis was performed using routine analytical methods (27). Lists of differentially expressed genes were controlled for false discovery rate (FDR) errors using the QValue method (28). Differentially expressed genes chosen for subsequent analysis met the following criteria: an FDR-corrected P value (called the q value) of $\leq$0.05, a minimum normalized expression level of $>$20-fold, and a minimum mean fluorescence signal intensity of $>$100 for either the NP or the AC replicate mean. The microarray data were submitted in Minimum Information About a Microarray Experiment (MIAME)–compliant format to the ArrayExpress database (online at www.mged.org/Workgroups/MIAME/miame.html; accession no. E-MEXP-2488).

Real-time quantitative polymerase chain reaction (PCR) analysis of articular cartilage and NP samples. Real-time quantitative PCR using gene-specific primers (Table 1) was performed on cDNA derived from NP and articular cartilage samples using the SYBR Green method as previously described (19). Five "normal" IVD samples (3 male and 2 female donors, ages 45–60 years [mean age 52 years]; histologic grade 1–3) and 5 "normal" articular cartilage samples (2 male and 3 female donors, ages 50–60 years [mean age 56 years]; histologic grade 1–2) were used for these analyses. The $2^{-\Delta C_t}$ method was used to calculate the relative expression of each target gene, as described previously (15,19,29). Statistical analysis was performed with GraphPad InStat software using the Mann-Whitney U test. P values less than 0.05 were considered significant.

BM-MSC and AD-MSC sample acquisition, isolation, and culture. Human BM-MSCs were isolated from bone marrow obtained from a proximal femur sample removed during hip replacement surgery from a 66-year-old man. The patient's informed consent and approval of the South Manchester Research Ethics Committee were obtained. Mononucleated cells were isolated using a Histopaque 1077 (Sigma) density-gradient method, and cultured in α-minimum essential medium (α-MEM) containing 20% fetal calf serum (FCS) to allow adherence. Nonadherent cells were discarded after 7 days, and the adherent cells were cultured using standard procedures.

Human AD-MSCs were isolated from adipose tissue obtained at surgery from a 38-year-old woman. The patient's consent and approval of the South Manchester Research Ethics Committee were obtained. Adipose tissue was dissected, suspended in Hanks' balanced salt solution containing 20 units of heparin and antibiotics, and centrifuged for 5 minutes at 500g. The resulting cell pellet was resuspended in α-MEM. Mononucleated cells were isolated, and the cells were cultured as described above for the BM-MSCs.

Table 2. Expression levels of previously described potential NP cell marker genes*

Gene description	Gene symbol	AC MFI	NP MFI	Fold difference (NP/AC)
Chondrogenic markers				
Type I collagen α1	*COL1A1*	201.28	218.04	1.08
Type II collagen α1	*COL2A1*	22,740.73	9,398.03	–2.42
Sex-determining region Y box 9	*SOX9*	2,618.06	3,260.23	1.25
Aggrecan	*ACAN*	18,543.37	11,543.32	–1.61
Versican	*VCAN*	196.75	1,983.43	10.08
Previously identified murine markers				
Keratin 19	*KRT19*	18.44	42.29	2.29
Glypican 3	*GPC3*	34.15	40.63	1.19
Annexin A3	*ANXA3*	15.79	14.66	–1.08
Pleiotrophin	*PTN*	399.96	52.16	–7.67
Vimentin	*VIM*	14,099.43	8,289.52	–1.70
Cartilage oligomeric matrix protein	*COMP*	26,678.53	18,915.58	–1.41
Previously identified canine markers				
Matrix Gla protein	*MGP*	17,602.04	2,356.78	–7.47
α_2-macroglobulin	*A2M*	5,320.54	4,415.59	–1.20
Annexin A4	*ANXA4*	1,482.17	953.32	–1.55
Desmocollin 2	*DSC2*	306.11	540.02	1.76
Keratin 18	*KRT18*	315.17	1,637.12	5.19
Neural cell adhesion molecule 1	*NCAM1*	165.85	234.02	1.41
Previously identified bovine markers				
Keratin 8	*KRT8*	140.69	95.71	–1.47
Cadherin 2, type 1, N-cadherin (neuronal)	*CDH2*	18.62	33.16	1.78
Synaptosomal-associated protein 25 kd	*SNAP25*	55.47	70.47	1.27
Sclerostin domain containing 1	*SOSTDC1*	21.26	24.18	1.14
Integrin-binding sialoprotein (bone sialoprotein 2)	*IBSP*	7,646.14	95.98	–79.66
Fibulin 1	*FBLN1*	166.12	97.65	–1.70
Tenomodulin	*TNMD*	21.65	24.36	1.13
Tumor necrosis factor α–induced protein 6	*TNFAIP6*	954.44	2,112.00	2.21
Forkhead box F1	*FOXF1*	39.01	1,837.78	47.11
Forkhead box F2	*FOXF2*	92.09	363.54	3.95
Aquaporin 1	*AQP1*	85.50	78.94	–1.08

* Values are the human microarray data for previously identified markers. For each cell type (nucleus pulposus [NP] cells and articular chondrocytes [ACs]), the mean values for the mean fluorescence intensity (MFI) of expression are shown, along with the calculated fold difference (positive and negative) between the NP cells and the ACs.

The multipotentiality of the BM-MSCs and AD-MSCs was verified using standard methods to confirm differentiation along the osteogenic, adipogenic, and chondrogenic lineages, in accordance with the guidelines of the International Society for Cellular Therapy (30) (data not shown).

Cells were seeded into type I collagen gels (Arthro-Kinetics) at a final density of 4×10^6 cells/ml. Seeded gels were formed in triplicate for both cell samples in 24-well cell culture inserts at a volume of 200 μl per gel and were cultured for 14 days under standard conditions in high-glucose Dulbecco's modified Eagle's medium (DMEM) containing 1% FCS, 1× ITS-X (insulin–transferrin–selenium X; Life Technologies), 1.25 mg/ml of bovine serum albumin (AlbuMax-1; Life Technologies), 100 units/ml of penicillin, 100 μg/ml of streptomycin, 250 ng/ml of amphotericin B, 100 μ*M* ascorbic acid 2-phosphate, 2 m*M* L-glutamine, $1 \times 10^7 M$ dexamethasone, and 10 ng/ml of transforming growth factor β1 (TGFβ1) (differentiating medium [15]). The medium was changed every 2–3 days.

Real-time quantitative PCR analysis of BM-MSCs and AD-MSCs. Following 14 days in culture, gels were digested for 2 hours in a solution of serum-free high-glucose DMEM containing 0.2% type II collagenase. Cells were collected by centrifugation, washed in phosphate buffered saline (PBS), and RNA was extracted and reverse transcribed to cDNA as described above. Real-time quantitative PCR was conducted for the housekeeping gene *GAPDH*, the standard marker genes *COL2A1* and *ACAN*, as well as a range of novel phenotype marker genes as described above.

Immunohistochemical analysis. Following 14 days in culture in differentiating medium, gels containing either BM-MSCs or AD-MSCs were washed in PBS, fixed in 4% paraformaldehyde, processed to paraffin wax embedding, and 5-μm sections were cut. Immunohistochemical staining was conducted for Forkhead box F1 (FoxF1), paired box protein 1 (Pax-1), carbonic anhydrase XII (CAXII), integrin-binding sialoprotein (IBSP), and fibulin 1, based on previously published protocols (31,32). Heat-mediated antigen retrieval was performed for 20 minutes using either 0.01*M* citrate buffer in a pressure cooker or 10 m*M* Tris, 1 m*M* EDTA, pH 9.0, in a steamer. Sections were incubated overnight at 4°C with primary antibodies for FoxF1 (rabbit polyclonal, 1:150 dilution; Abcam), Pax-1 (rabbit polyclonal, 1:50 dilution; Novus Biologicals), CAXII (rabbit polyclonal, 1:50 dilution; Sigma-Aldrich),

Table 3. Comparison of NP versus AC microarray data*

Gene description	Gene symbol	NP MFI	AC MFI	Fold difference (NP/AC)
Ovostatin 2†	*OVOS2*	2,426.58	27.70	87.60
Class II major histocompatibility complex DQβ1	*HLA–DQB1*	2,803.04	46.19	60.68
Hemoglobin α1-chain	*HBA1*	5,284.22	92.82	56.93
Hemoglobin β-chain†	*HBB*	2,001.62	35.91	55.74
Forkhead box F1†‡	*FOXF1*	1,837.78	39.01	47.11
Carbonic anhydrase XII†	*CA12*	2,726.90	71.33	38.23
ATP-binding cassette subfamily G member 1	*ABCG1*	739.68	20.30	36.44
Family with sequence similarity 110 member C	*FAM110C*	1711.45	48.98	34.94
Paired box 1†	*PAX1*	1,638.17	51.71	31.68
Zinc-finger protein 165	*ZNF165*	1,136.78	36.94	30.77
Double cortin–like kinase 1	*DCLK1*	655.18	23.23	28.21
Annexin A2	*ANXA2*	380.79	18.48	20.61
Matrilin 3	*MATN3*	13.00	481.92	–37.08
Tenascin C	*TNC*	159.40	6,436.00	–40.38
Cytokine-like 1†	*CYTL1*	345.59	14,174.13	–41.01
Spondin 1, extracellular matrix protein	*SPON1*	42.78	1,784.01	–41.70
Kallmann syndrome 1 sequence	*KAL1*	57.96	2,612.33	–45.07
G protein–coupled receptor 88	*GPR88*	14.37	677.60	–47.16
Complement factor H	*CFH*	3,31.57	16,879.22	–50.91
Collectin subfamily member 12	*COLEC12*	47.87	2,956.07	–61.75
Integrin-binding sialoprotein (bone sialoprotein 2)†‡	*IBSP*	95.98	7,646.14	–79.66
Epidermal growth factor–containing fibulin-like extracellular matrix protein 1	*EFEMP1*	71.55	6,149.25	–85.94
Vascular cell adhesion molecule 1	*VCAM1*	52.66	5,065.74	–96.20
Growth differentiation factor 10†	*GDF10*	43.32	4,262.62	–98.39

* For each cell type (nucleus pulposus [NP] cells and articular chondrocytes [ACs]), the mean values for the mean fluorescence intensity (MFI) of expression are shown, along with the calculated fold difference (positive and negative) between the NP cells and the ACs.
† Analyzed by real-time quantitative reverse transcription–polymerase chain reaction.
‡ Identified in previously published microarray studies (17–20).

IBSP (rabbit polyclonal, 1:50 dilution; Abcam), and fibulin 1 (mouse monoclonal, 1:25 dilution; Santa Cruz Biotechnology). Biotinylated goat anti-rabbit and goat anti-mouse secondary antibodies were used, and staining was disclosed using a diaminobenzidine chromogen. Negative controls used the appropriate IgG (Dako) in place of the primary antibody at equal protein concentrations. Stained sections were viewed under light microscopy, and images were acquired using an InfinityX camera with DeltaPix software.

RESULTS

Microarray analysis of previously identified "marker" genes. Typical chondrocyte markers were used to evaluate the ability of the microarrays to detect gene expression in the 2 cell types (Table 2). Expected patterns of expression were seen for *COL2A1*, *SOX9*, and *ACAN*, which were detected at high levels in both NP and AC samples. For comparative purposes, a number of genes that were identified in previous microarray experiments as being phenotype NP markers of murine (18), canine (20), and bovine (19) cells were assessed to determine their expression in human arrays.

The murine NP cell markers *KRT19*, *GPC3*, *ANXA3*, and *PTN* were detected at low levels in our human NP cell arrays; *VIM* and *COMP* were detected in the arrays at high levels in both NP and AC cells, suggesting their unsuitability as marker genes in human NP cells.

Of the canine markers identified, only *KRT18* showed significant differential expression (5-fold) in NP cells as compared with ACs. *MGP* was differentially expressed in ACs (~7-fold) as compared with NP cells, but was also detected at significant levels in NP cells; therefore, *MGP* is unlikely to distinguish the two cell types. None of the other reported canine genes (*A2M*, *ANXA4*, *DSC2*, and *NCAM1*) showed any significant fold differences in expression between the two cell types.

Similarly, a significant number of the markers identified in the bovine arrays showed relatively low differential expression in human NP cells versus ACs, such as *KRT8*, *CDH2*, *SNAP25*, *SOSTDC1*, *TNMD*, and *AQP1*. Two bovine genes showed particularly high levels of differential expression in the human arrays. The bovine IVD marker *FOXF1* showed a 47-fold increased expression in NP cells as compared with ACs, and the bovine AC marker *IBSP* showed an ~80-fold increase in expression in ACs as compared with NP cells (Table 2).

Microarray identification of novel cell-specific "marker" genes. To identify additional novel genes that could be used to distinguish human NP cells from ACs, the average expression levels in NP cells were compared with the average expression levels in ACs (NP mean/AC mean). Differentially expressed genes met the following criteria: an FDR-corrected *P* value (called the q value) of ≤0.05, a minimum normalized expression level of >20-fold, and a minimum mean fluorescence signal intensity of >100 for either the NP cell or the AC replicate mean. Using these criteria, a total of 64 probe sets (48 genes) were identified, of which 12 genes showed high levels of differential expression in NP cells and 36 genes showed high levels of differential expression in ACs. Table 3 highlights the 24 most differentially expressed genes for both NP cells (12 genes) and ACs (12 genes). Genes that were analyzed by real-time quantitative PCR and genes that were identified in previously published microarray studies (17–20) are indicated in Table 3.

The serine protease inhibitor *OVOS2* showed the highest level of differential expression in NP cells and was selected for analysis by real-time quantitative PCR. Other highly expressed genes, including the oxygen-transport metalloprotein gene *HBB*, the carbon dioxide–transport metalloenzyme gene *CA12*, the transcription factor gene *PAX1*, and the previously identified NP marker *FOXF1*, were also further examined by real-time quantitative PCR analysis. The TGFβ superfamily member gene *GDF10*, which was the highest differentially expressed gene in ACs, was selected for real-time quantitative PCR analysis, along with the highly expressed *CYTL1* gene, and these were analyzed with the previously identified *IBSP* and *FBLN1* genes (19).

Real-time quantitative PCR validation of cell-specific marker genes in human samples. Real-time quantitative PCR demonstrated high levels of both *COL2A1* and *ACAN* in NP cells and ACs, although the gene expression levels were lower in NP cells than in ACs ($P < 0.0001$ for both genes) (data not shown).

The novel NP markers all showed significantly higher expression in NP cells as compared with ACs (Figure 1A). The most significant of these was *PAX1*, which showed >1,000-fold higher levels of expression in NP cells than in ACs ($P < 0.0001$). The previously identified transcription factor gene *FOXF1* was also found to have significantly higher levels of expression in NP cells than in ACs (>50-fold; $P < 0.0001$). In addition, *CA12* and *HBB* showed significantly higher levels of expression in NP cells than in ACs (>50-fold [$P < 0.0001$] and >100-fold [$P < 0.0001$], respectively).

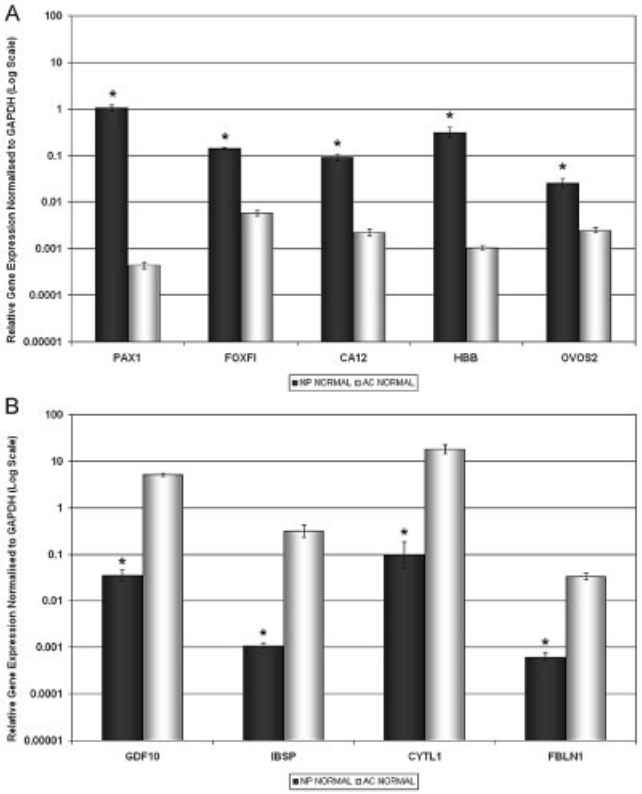

Figure 1. Real-time quantitative polymerase chain reaction analysis of **A,** the novel positive nucleus pulposus (NP) cell marker genes *PAX1*, *FOXF1*, *CA12*, *HBB*, and *OVOS2*, and **B,** the novel NP-negative cell marker genes *GDF10*, *IBSP*, *CYTL1*, and *FBLN1* in human NP cells and articular chondrocytes (ACs). The relative gene expression for all marker genes was normalized to the housekeeping gene *GAPDH* and plotted on a log scale. Values are the mean ± SEM. * = $P < 0.05$ versus ACs.

OVOS2 gene expression was significantly lower in ACs than in NP cells ($P < 0.0001$), although the overall fold difference between NP cells and ACs (~10-fold) was considerably lower than that detected by the array (87-fold).

The previously identified NP-negative markers *IBSP* and *FBLN1* showed low expression in NP cells, with significantly higher expression in ACs (>100-fold [$P < 0.0001$] and >50-fold [$P < 0.0001$], respectively) (Figure 1B). Expression of *GDF10* and *CYTL1* genes was significantly higher (>100 fold; $P < 0.0001$) in ACs than in NP cells, although the expression levels in NP cells were higher than that of either *IBSP* or *FBLN1*.

Differentiation of BM-MSCs and AD-MSCs to an NP-like phenotype. Following culture in type I collagen gels, both AD-MSCs and BM-MSCs demonstrated significant increases in the classic marker genes *COL2A1*

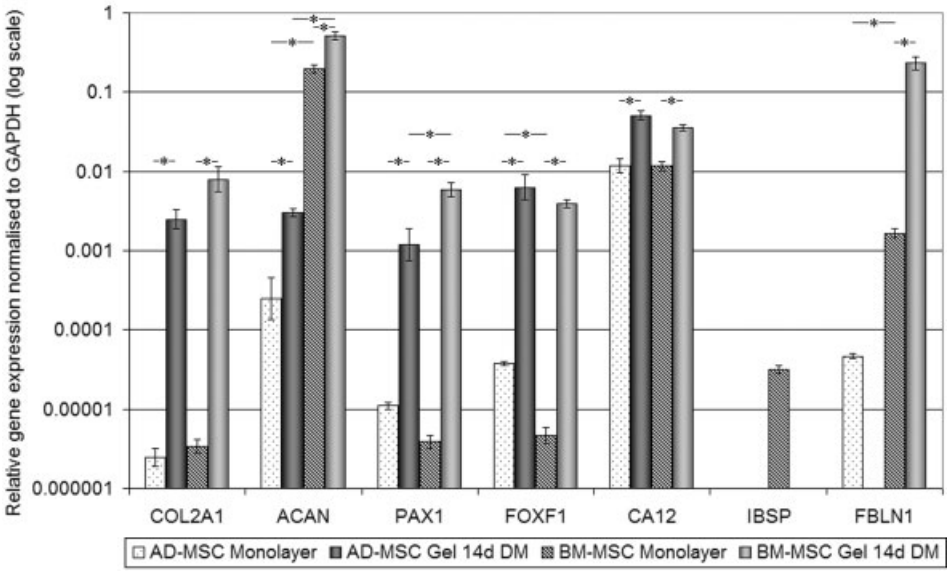

Figure 2. Real-time quantitative polymerase chain reaction analysis of the novel nucleus pulposus (NP) cell and articular chondrocyte (AC) markers *COL2A1*, *ACAN*, *PAX1*, *FOXF1*, *CA12*, *IBSP*, and *FBLN1* in monolayer and differentiated human adipose tissue–derived mesenchymal stem cells (AD-MSCs) and bone marrow–derived mesenchymal stem cells (BM-MSCs). Cells were obtained from monolayer cultures or were obtained on day 14 from type I collagen gel cultures in differentiating medium (DM) (see Materials and Methods for details). Relative gene expression was normalized to the housekeeping gene *GAPDH* and plotted on a log scale. Values are the mean ± SEM. $* = P < 0.05$.

and *ACAN*. Expression of the novel NP marker genes *PAX1* and *FOXF1* was also significantly increased in both AD-MSCs and BM-MSCs as compared with monolayer controls. There were also significant increases in the *CA12* gene in both cell types, although basal levels in both AD-MSCs and BM-MSCs were high during monolayer culture as compared with the other genes investigated. Interestingly, AD-MSCs lacked expression of the negative marker gene IBSP, both in monolayer culture and following culture in type I collagen gels, whereas although BM-MSCs expressed this gene in monolayer culture, there was no expression following culture in type I collagen gels. *FBLN1* was expressed in both monolayer AD-MSCs and BM-MSCs, with significantly higher expression seen in monolayer BM-MSCs. However, following type I collagen gel culture, although *FBLN1* gene expression significantly increased in BM-MSCs as compared with expression in monolayer culture, no expression of this gene was detected in AD-MSCs cultured in type I collagen gels for 14 days in differentiating medium (Figure 2).

When protein expression in AD-MSCs and BM-MSCs was analyzed following culture in type I collagen gels, both cell types demonstrated similar levels of immunopositivity for type II collagen α1, aggrecan, and CAXII (data not shown). However, AD-MSCs demonstrated strong cellular staining for Pax-1 and FoxF1 as compared with staining of BM-MSCs under the same conditions (Figure 3). AD-MSCs also demonstrated virtually no cellular staining for either IBSP or fibulin 1, whereas BM-MSCs demonstrated immunopositivity for both negative NP markers. All IgG controls were negative.

DISCUSSION

NP cells of the IVD share a common phenotype with ACs, as demonstrated by the expression of the key chondrocyte genes *COL2A1*, *ACAN*, and *SOX9* in both cell types (14). However, there are clear morphologic and physiologic differences between articular cartilage and NP tissues that suggest differences in the 2 cell phenotypes. In addition to offering a greater understanding of cell biology, the identification of the exact NP cell phenotype is essential for tissue engineering/regenerative therapies for IVD degeneration.

The exact phenotype of the human NP cell is largely unknown, although several recent studies have

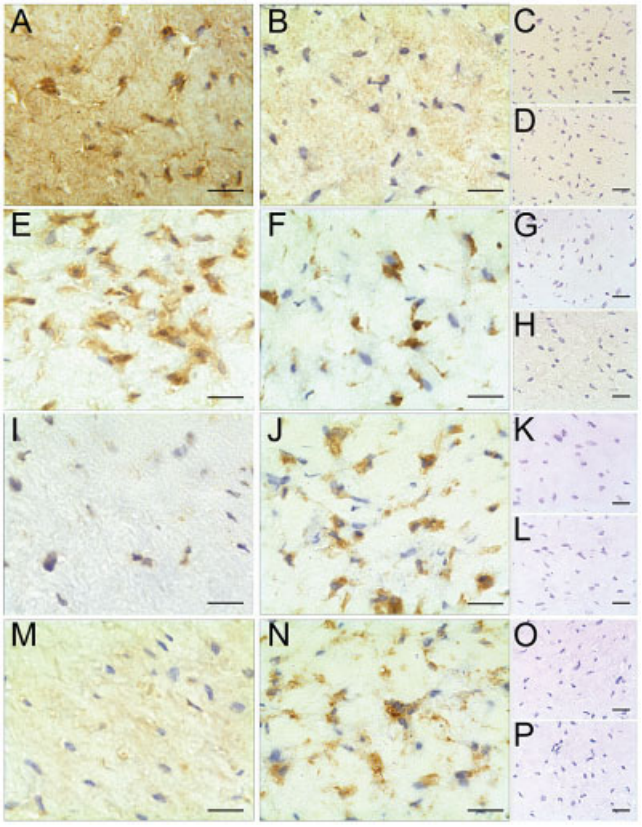

Figure 3. Immunohistochemical staining for novel nucleus pulposus (NP) cell and articular chondrocyte (AC) markers in human adipose tissue–derived mesenchymal stem cells (AD-MSCs) and bone marrow–derived mesenchymal stem cells (BM-MSCs) cultured in type I collagen gels in differentiating medium for 14 days. Photomicrographs represent typical staining patterns for the NP markers paired box protein 1 (Pax-1) in AD-MSCs (**A**) and BM-MSCs (**B**) and Forkhead box F1 (FoxF1) in AD-MSCs (**E**) and BM-MSCs (**F**), as well as for the AC markers integrin-binding sialoprotein (IBSP) in AD-MSCs (**I**) and BM-MSCs (**J**) and fibulin 1 in AD-MSCs (**M**) and BM-MSCs (**N**) following culture in type I collagen gels. IgG controls were routinely negative in both AD-MSCs (**C**, **G**, **K**, and **O**) and BM-MSCs (**D**, **H**, **L**, and **P**). Bars = 25 μm.

attempted to elucidate differences in the transcription profiles between ACs and NP cells in rats, cows, and dogs (18–20). Here, we have used Affymetrix MicroArrays and real-time quantitative PCR to identify genes that can be used to distinguish human NP cells from ACs. Furthermore, we have demonstrated that these marker genes can be used to identify the in vitro differentiation of BM-MSCs and AD-MSCs to an NP-like phenotype in biomaterials suitable for tissue engineering/regeneration of the human IVD.

This study is the first to use microarray technology to examine human NP cells and ACs, and a number of differentially expressed novel genes in human NP cells as compared with ACs were identified. Importantly, several differentially expressed genes identified from microarray studies in other animals (e.g., *GPC3* and *KRT19* from murine, *A2M* and *ANXA4* from canine, and *KRT18* and *CDH2* from bovine studies) did not translate directly to this human study, with limited differential expression detected between the 2 cell types. This may be due to differences in disc age, size, native cell composition, and the physicochemical environment in these animal species was compared with the human lumbar discs. Furthermore, although macroscopically and histologically normal tissues were used for this study to avoid phenotype changes caused by degeneration, the AC cells were nevertheless derived from "normal" regions of OA joints, and thus, their gene profile could be different from that of non-OA cartilage. Interestingly however, the previously identified bovine NP marker *FOXF1* and the AC marker/NP-negative marker *IBSP* (19) were also highly differentially expressed in the human arrays, and these findings were confirmed by real-time quantitative PCR in human NP cells and ACs. Such data demonstrate the existence of positive (NP) and negative (AC) markers between species and suggest that these 2 genes are potential marker genes for differentiating NP cells from ACs in both bovine and human tissues.

In addition, several novel human markers were identified in the microarray analysis, including the novel NP markers *PAX1*, *CA12*, and *HBB* and were validated by real-time quantitative PCR, with *PAX1* having a particularly high differential expression between the 2 tissue types (>1,000 fold; $P < 0.0001$). The array analyses also identified novel AC markers *GDF10* and *CYTL1*, which were confirmed by real-time quantitative PCR as being expressed >100-fold higher in ACs than in NP cells ($P < 0.0001$), and thus may serve (together with *IBSP* and *FBLN1* identified from our bovine studies [19]), as negative markers for the NP phenotype.

Although previously identified in the IVDs of young adult mice (33) and in the human fetal vertebral column (34), this is the first time that *PAX1* expression has been demonstrated in the adult human IVD. *PAX1* encodes a transcription factor that regulates pattern formation during embryogenesis in vertebrates (35). Its expression is regulated by *SHH*, which has been shown to be expressed in the embryonic sclerotome and in the postnatal mouse NP (36,37); however, its role in the adult human NP remains to be elucidated. Interestingly, *FOXF1* expression has also been shown to be activated by *SHH*, and while the role of *FOXF1* in cell growth,

proliferation, differentiation, and longevity (38–40) has been established, its role in the adult human IVD has yet to be understood.

The high levels of expression of hemoglobin chains (*HBB* and *HBA1*) and *CA12* in NP cells suggests that the harsh, hypoxic environment of the IVD significantly influences gene expression of resident cells. The oxygen-transport metalloprotein hemoglobin, which is found in red blood cells, has been recently detected in a number of nonerythroid cells, including dopaminergic neurons, macrophages, alveolar cells, and mesangial cells of the kidney (41–43). It is thought to act by storing oxygen, and it thereby provides a homeostatic mechanism under hypoxic conditions for metabolically active cells. Similarly, the zinc-containing metalloenzyme CAXII, which catalyzes the reversible hydration of carbon dioxide and is responsible for the maintenance of body ion and pH homeostasis (42), is regulated by hypoxia-inducible factor 1α (HIF-1α) under hypoxic conditions (44), and other CA family members have been identified in the fetal human IVD (45). It is therefore likely that these genes are highly expressed in NP cells in order to maintain homeostasis in the avascular, hypoxic, nutrient-deprived, and acidic environment of the adult human IVD.

There is increasing interest in the potential use of adult stem cells in tissue engineering strategies for regenerating the degenerated human IVD. Both BM-MSCs and AD-MSCs are known to be capable of chondrogenic differentiation (46,47), and recent studies have demonstrated their potential for use in IVD tissue regeneration (11–13). Such studies have routinely used chondrocyte marker genes such as *SOX9*, *COL2A1*, and *ACAN* to identify the differentiation of BM-MSCs or AD-MSCs to NP-like cells. However, evidence suggests that implantation of chondrocyte-like cells, which do not have the correct NP cell phenotype, will result in the formation of a tissue that does not mimic the highly hydrated NP, and therefore lacks the morphologic or biomechanical properties, to ensure successful regeneration of a functional IVD (48). To overcome this problem, we used the novel marker genes identified in this study in a small proof-of-principle study to assess differentiation to an appropriate NP phenotype.

While both BM-MSCs and AD-MSCs have similar cell surface marker profiles, during monolayer culture, differences in the gene expression profiles between the 2 cell populations suggested that there was a difference in the initial phenotype that may affect their subsequent differentiation to NP cells.

Following differentiation in type I collagen gels, both BM-MSCs and AD-MSCs demonstrated significant up-regulation in expression of the conventional NP marker genes. Importantly, both cell types also demonstrated large and significant increases in expression of the novel NP marker genes *PAX1* and *FOXF1* as well as small but significant increases in *CA12*, while immunohistochemical staining suggested more marked and widespread expression of both Pax-1 and FoxF1 in AD-MSCs than in BM-MSCs. Significantly, differentiated AD-MSCs did not express the negative NP markers *IBSP* or *FBLN1* at either the gene or the protein level, whereas BM-MSCs expressed *FBLN1* at both the gene and the protein levels and expressed the IBSP protein. Expression of IBSP at the protein level may be due to the high levels of IBSP RNA observed in monolayer culture, which may not be immediately down-regulated under differentiating conditions.

These preliminary results, albeit on a small number of samples, suggest that the novel marker genes identified here may be used to characterize NP-specific differentiation of adult stem cells. Interestingly, while both BM-MSCs and AD-MSCs are capable of chondrogenic differentiation, AD-MSCs differentiate to a more NP-like phenotype than do BM-MSCs and may therefore be more suited to IVD tissue engineering strategies.

ACKNOWLEDGMENTS

We would like to acknowledge Mr. Adam Dickinson, who assisted with the stem cell cultures, and Miss Francesca Ludwinski, Miss Sonal Patel, and Mrs. Pauline Baird, who helped with antibody optimizations. Array hybridizations and initial analyses were performed by staff at the Microarray and Bioinformatics Core Facilities, Faculty of Life Sciences, University of Manchester.

AUTHOR CONTRIBUTIONS

All authors were involved in drafting the article or revising it critically for important intellectual content, and all authors approved the final version to be published. Prof. Hoyland had full access to all of the data in the study and takes responsibility for the integrity of the data and the accuracy of the data analysis.

Study conception and design. Minogue, Richardson, Zeef, Freemont, Hoyland.

Acquisition of data. Minogue, Richardson, Zeef.

Analysis and interpretation of data. Minogue, Richardson, Zeef, Hoyland.

REFERENCES

1. Walker BF. The prevalence of low back pain: a systematic review of the literature from 1966 to 1998. J Spinal Disord 2000;13: 205–17.
2. Crow WT, Willis DR. Estimating cost of care for patients with

acute low back pain: a retrospective review of patient records. J Am Osteopath Assoc 2009;109:229–33.
3. Buckwalter JA. Aging and degeneration of the human intervertebral disc. Spine 1995;20:1307–14.
4. Luoma K, Riihimaki H, Luukkonen R, Raininko R, Viikari-Juntura E, Lamminen A. Low back pain in relation to lumbar disc degeneration. Spine 2000;25:487–92.
5. Pearce RH, Grimmer BJ, Adams ME. Degeneration and the chemical composition of the human lumbar intervertebral disc. J Orthop Res 1987;5:198–205.
6. Li X, Lee JP, Balian G, Greg AD. Modulation of chondrocytic properties of fat-derived mesenchymal cells in co-cultures with nucleus pulposus. Connect Tissue Res 2005;46:75–82.
7. Lu ZF, Zandieh DB, Wuisman PI, Bank RA, Helder MN. Differentiation of adipose stem cells by nucleus pulposus cells: configuration effect. Biochem Biophys Res Commun 2007;359: 991–6.
8. Richardson SM, Hughes N, Hunt JA, Freemont AJ, Hoyland JA. Human mesenchymal stem cell differentiation to NP-like cells in chitosan-glycerophosphate hydrogels. Biomaterials 2008;29:85–93.
9. Risbud MV, Albert TJ, Guttapalli A, Vresilovic EJ, Hillibrand AS, Vaccaro AR, et al. Differentiation of mesenchymal stem cells towards a nucleus pulposus-like phenotype in vitro: implications for cell-based transplantation therapy. Spine 2004;29:2627–32.
10. Steck E, Bertram H, Abel R, Chen B, Winter A, Richter W. Induction of intervertebral disc-like cells from adult mesenchymal stem cells. Stem Cells 2005;23:403–11.
11. Ganey T, Hutton WC, Moseley T, Hedrick M, Meisel HJ. Intervertebral disc repair using adipose tissue-derived stem and regenerative cells: experiments in a canine model. Spine 2009;34: 2297–304.
12. Hiyama A, Mochida J, Iwashina T, Omi H, Watanabe T, Serigano K, et al. Transplantation of mesenchymal stem cells in a canine disc degeneration model. J Orthop Res 2008, 26:589–600.
13. Sakai D, Mochida J, Iwashina T, Watanabe T, Nakai T, Ando K, et al. Differentiation of mesenchymal stem cells transplanted to a rabbit degenerative disc model: potential and limitations for stem cell therapy in disc regeneration. Spine 2005;30:2379–87.
14. Sive JI, Baird P, Jeziorsk M, Watkins A, Hoyland JA, Freemont AJ. Expression of chondrocyte markers by cells of normal and degenerate intervertebral discs. Mol Pathol 2002;55:91–7.
15. Richardson SM, Curran JM, Chen R, Vaughan-Thomas A, Hunt JA, Freemont AJ, et al. The differentiation of bone marrow mesenchymal stem cells into chondrocyte-like cells on poly-L-lactic acid (PLLA) scaffolds. Biomaterials 2006;27: 4069–78.
16. Tsai TT, Guttapalli A, Oguz E, Chen LH, Vaccaro AR, Albert TJ, et al. Fibroblast growth factor-2 maintains the differentiation potential of nucleus pulposus cells in vitro: implications for cell-based transplantation therapy. Spine 2007;32:495–502.
17. Fujita N, Miyamoto T, Imai J, Hosogane N, Suzuki T, Yagi M, et al. CD24 is expressed specifically in the nucleus pulposus of intervertebral discs. Biochem Biophys Res Commun 2005;338: 1890–6.
18. Lee CR, Sakai D, Nakai T, Toyama K, Mochida J, Alini M, et al. A phenotypic comparison of intervertebral disc and articular cartilage cells in the rat. Eur Spine J 2007;16:2174–85.
19. Minogue BM, Richardson SM, Zeef LA, Freemont AJ, Hoyland JA. Transcriptional profiling of bovine intervertebral disc cells: implications for identification of normal and degenerate human intervertebral disc cell phenotypes. Arthritis Res Ther 2010;12: R22.
20. Sakai D, Nakai T, Mochida J, Alini M, Grad S. Differential phenotype of intervertebral disc cells: microarray and immunohistochemical analysis of canine nucleus pulposus and anulus fibrosus. Spine 2009;34:1448–56.
21. Gilson A, Dreger M, Urban JP. Differential expression levels of cytokeratin 8 in cells of the bovine nucleus pulposus complicates the search for specific intervertebral disc cell markers. Arthritis Res Ther 2010;12:R24.
22. Rutges J, Creemers LB, Dhert W, Milz S, Sakai D, Mochida J, et al. Variations in gene and protein expression in human nucleus pulposus in comparison with annulus fibrosus and cartilage cells: potential associations with aging and degeneration. Osteoarthritis Cartilage 2010;18:416–23.
23. Mankin HJ, Dorfman H, Lippiello L, Zarins A. Biochemical and metabolic abnormalities in articular cartilage from osteo-arthritic human hips. II. Correlation of morphology with biochemical and metabolic data. J Bone Joint Surg Am 1971;53:523–7.
24. Thomas CM, Fuller CJ, Whittles CE, Sharif M. Chondrocyte death by apoptosis is associated with cartilage matrix degradation. Osteoarthritis Cartilage 2007;15:27–34.
25. Li C, Wong WH. Model-based analysis of oligonucleotide arrays: expression index computation and outlier detection. Proc Natl Acad Sci U S A 2001;98:31–6.
26. Bolstad BM, Irizarry RA, Astrand M, Speed TP. A comparison of normalization methods for high density oligonucleotide array data based on variance and bias. Bioinformatics 2003;19:185–93.
27. Smyth GK. Linear models and empirical Bayes methods for assessing differential expression in microarray experiments. Stat Appl Genet Mol Biol 2004;3:article 3.
28. Storey JD, Tibshirani R. Statistical significance for genomewide studies. Proc Natl Acad Sci U S A 2003;100:9440–5.
29. Livak KJ, Schmittgen TD. Analysis of relative gene expression data using real-time quantitative PCR and the $2^{-\Delta\Delta C_T}$ method. Methods 2001;25:402–8.
30. Dominici M, Le Blanc K, Mueller I, Slaper-Cortenbach I, Marini F, Krause D, et al. Minimal criteria for defining multipotent mesenchymal stromal cells: the International Society for Cellular Therapy position statement. Cytotherapy 2006;8:315–7.
31. Le Maitre CL, Freemont AJ, Hoyland JA. Localization of degradative enzymes and their inhibitors in the degenerate human intervertebral disc. J Pathol 2004;204:47–54.
32. Pockert AJ, Richardson SM, Le Maitre CL, Lyon M, Deakin JA, Buttle DJ, et al. Modified expression of the ADAMTS enzymes and tissue inhibitor of metalloproteinases 3 during human intervertebral disc degeneration. Arthritis Rheum 2009; 60:482–91.
33. DiPaola CP, Farmer JC, Manova K, Niswander LA. Molecular signaling in intervertebral disk development. J Orthop Res 2005; 23:1112–9.
34. Smith CA, Tuan RS. Functional involvement of Pax-1 in somite development: somite dysmorphogenesis in chick embryos treated with Pax-1 paired-box antisense oligodeoxynucleotide. Teratology 1995;52:333–45.
35. McGaughran JM, Oates A, Donnai D, Read AP, Tassabehji M. Mutations in PAX1 may be associated with Klippel-Feil syndrome. Eur J Hum Genet 2003;11:468–74.
36. Dahia CL, Mahoney EJ, Durrani AA, Wylie C. Intercellular signaling pathways active during intervertebral disc growth, differentiation, and aging. Spine 2009;34:456–62.
37. Koseki H, Wallin J, Wilting J, Mizutani Y, Kispert A, Ebensperger C, et al. A role for Pax-1 as a mediator of notochordal signals during the dorsoventral specification of vertebrae. Development 1993;119:649–60.
38. Kalinichenko VV, Zhou Y, Bhattacharyya D, Kim W, Shin B, Bambal K, et al. Haploinsufficiency of the mouse Forkhead Box f1 gene causes defects in gall bladder development. J Biol Chem 2002;277:12369–74.
39. Mahlapuu M, Ormestad M, Enerback S, Carlsson P. The forkhead transcription factor Foxf1 is required for differentiation of extra-embryonic and lateral plate mesoderm. Development 2001;128: 155–66.

40. Ormestad M, Astorga J, Landgren H, Wang T, Johansson BR, Miura N, et al. Foxf1 and Foxf2 control murine gut development by limiting mesenchymal Wnt signaling and promoting extracellular matrix production. Development 2006;133:833–43.
41. Liu L, Zeng M, Stamler JS. Hemoglobin induction in mouse macrophages. Proc Natl Acad Sci U S A 1999;96:6643–7.
42. Newton DA, Rao KM, Dluhy RA, Baatz JE. Hemoglobin is expressed by alveolar epithelial cells. J Biol Chem 2006;281: 5668–76.
43. Nishi H, Inagi R, Kato H, Tanemoto M, Kojima I, Son D, et al. Hemoglobin is expressed by mesangial cells and reduces oxidant stress. J Am Soc Nephrol 2008;19:1500–8.
44. Wykoff CC, Beasley NJ, Watson PH, Turner KJ, Pastorek J, Sibtain A, et al. Hypoxia-inducible expression of tumor-associated carbonic anhydrases. Cancer Res 2000;60:7075–83.
45. Liao SY, Lerman MI, Stanbridge EJ. Expression of transmembrane carbonic anhydrases, CAIX and CAXII, in human development. BMC Dev Biol 2009;9:22.
46. Lee RH, Kim B, Choi I, Kim H, Choi HS, Suh K, et al. Characterization and expression analysis of mesenchymal stem cells from human bone marrow and adipose tissue. Cell Physiol Biochem 2004;14:311–24.
47. Puetzer JL, Petitte J, Loboa EG. Comparative review of growth factors for induction of three-dimensional in vitro chondrogenesis in human mesenchymal stem cells isolated from bone marrow and adipose tissue. Tissue Eng Part B Rev 2010;16:435–44.
48. Gorensek M, Jaksimovic C, Kregar-Velikonja N, Gorensek M, Knezevic M, Jeras M, et al. Nucleus pulposus repair with cultured autologous elastic cartilage derived chondrocytes. Cell Mol Biol Lett 2004;9:363–73.